

OGLE small amplitude red giant variables in the Galactic Bar

J. J. Wray,¹ L. Eyer^{1,2*} & B. Paczynski¹

¹ *Princeton University Observatory, Princeton, NJ 08544-1001, USA*

² *Observatoire de Genève, CH-1290 Sauverny, Switzerland*

2 February 2008

ABSTRACT

Among over 200,000 Galactic Bulge variable stars in the public domain OGLE catalogue, we found over 15,000 red giant variables following two well defined period – amplitude relations. The periods are in the range $10 < P < 100$ days, and amplitudes in the range $0.005 < A < 0.13$ mag in I-band. The variables cover a broad range of reddening corrected colours, $1 < (V - I)_0 < 5$, and a fairly narrow range of extinction corrected apparent magnitudes, $10.5 < I_0 < 13$. A subset of variables (type A) has a rms scatter of only 0.44 mag. The average magnitudes for these stars are well correlated with the Galactic longitude, and vary from $I_{k,0} = 11.82$ for $l = +8^\circ$ to $I_{k,0} = 12.07$ for $l = -5^\circ$, clearly indicating that they are located in the Galactic Bar. Most variables have several oscillation periods.

Key words: Galaxy:Bulge – stars:variables

1 INTRODUCTION

While the existence of the Galactic Bar was pointed out decades ago (de Vaucouleurs 1964), the Bar existence received a broader support only following the work of Blitz & Spergel (1991), based on 2.4 micron light distribution in the inner Galaxy as measured by Matsumoto et al. (1982), and the work of Nakada et al. (1991), based on the asymmetry in the distribution of Galactic Bulge stars as measured by IRAS. The presence of the Galactic Bar has been observed in many different ways; recent reviews are provided by Garzón (1999), Gerhard (2002), Dehnen (2002), and Merrifield (2003).

The Optical Gravitational Lensing Experiment (OGLE) is a long term observing project carried out at the Las Campanas Observatory in Chile, operated by the Carnegie Institution of Washington. The instrumentation of the three stages of the project was described by Udalski et al. (1992, OGLE-I), Udalski et al. (1997, OGLE-II), and Udalski et al. (2002a, OGLE-III). A catalogue of over 200,000 variable stars discovered within approximately 11 square degrees in the direction of the Galactic Bulge was published by Woźniak et al. (2001). The public domain data set contains 200 – 400 I-band photometric data points obtained in the observing seasons 1997, 1998, 1999 with the OGLE-II instrumentation: a dedicated 1.3-meter telescope with a $2K \times 2K$ pixel CCD camera, built and operated by the Warsaw University Observatory.

The presence of the Galactic Bar was already detected in the apparent distribution of red clump giants in the OGLE-I data (Stanek et al. 1994, Stanek et al. 1997). In this paper, we set out to determine whether the evidence for the Galactic Bar may also be found among OGLE variables. We calculated periodograms (Lomb 1976, Press et al. 1992) for each of the 200,000 objects in the OGLE-II variable star catalogue (Woźniak et al. 2001) that had at least 100 I-band measurements, and accepted as real those for which the probability of a false signal (Press et al. 1992) was smaller than 0.001. Because fields 45 and 46 have only two seasons of observations (fewer than 100 measurements), periodograms were not calculated for any stars in these fields. We were struck by the two clear sequences apparent in the period – amplitude diagram, presented in Fig. 1. For many stars, several significant periods were found. The plotted period has the largest amplitude. Our convention is that amplitudes are defined as half of the peak-to-peak amplitude for a given mode.

Originally, we had intended to use Mira-type long period variables as possible tracers of the Galactic Bar. However, it is clear that the variables defining the two sequences in Fig. 1 are more numerous and, having small amplitudes, they appear to be more useful than Miras as tracers of the Galactic structure. Therefore, this paper is devoted to these low amplitude variables only.

In addition to the two sequences present in Fig. 1 there is a clump of variables around $\log P \sim 2.1$ and $\log A < -2$; this is mostly caused by an artefact, and should be ignored.

We divided the variables into types A and B, with the

* E-mail: laurent.eyer@obs.unige.ch

division line shown in Fig. 1. Type A is above and to the left, and type B below and to the right, of the division line. Variables within the parallelograms:

$$\begin{aligned} -2.31 &< \log(A) < -1.31, \\ -6.56 &< \log(A) - 3.223 \log(P) < -5.66, \end{aligned} \quad (1a)$$

$$\begin{aligned} -1.82 &< \log(A) < -0.90, \\ -7.62 &< \log(A) - 3.223 \log(P) < -6.56, \end{aligned} \quad (1b)$$

were selected in 33 OGLE-II fields spanning a large range of Galactic longitudes, but only a small range of Galactic latitudes. The colour – magnitude diagram, corrected for interstellar reddening and extinction with the maps provided by Sumi (2003), is shown in Fig. 2 for the field BUL_SC1. Type A variables are marked with large blue dots; B variables are marked with green open circles. A relatively small range of apparent I-band magnitudes and a large number of variables indicates that these stars might be useful ‘standard candles,’ and that it might be possible to use them as tracers of the Galactic Bar.

Most variables shown in Fig. 2 are bright red giants. It is very likely that these stars are similar to the variables found by Kiss & Bedding (2003) and Ita et al. (2003) in the OGLE catalogue for the LMC and SMC, to those found by Cook et al. (1997), Wood et al. (1999), and Wood (2000) in the MACHO database for the LMC, to the M giant variables in NGC 6522 (Glass & Schultheis 2003), and to those found by Cook et al. (1997) in the MACHO database for the Galactic Bulge. Minimum variability levels have been detected for red giants from the ESO project “long term photometry on variables” (Jorissen et al. 1997), and also from Hipparcos photometry (Eyer & Grenon 1997), the cooler stars having larger minimum variability thresholds and larger mean amplitudes. Furthermore, a period-amplitude relation has been noticed for a few red giants stars by Jorissen et al. (1997), and also in a large sample of stars from ASAS data (Eyer & Blake 2002). A possible theoretical mechanism for the oscillations was studied by Dziembowski et al. (2001) and Christensen-Dalsgaard et al. (2001).

The aim of our paper is to select from the OGLE catalogue red giant variables populating the two period – amplitude sequences in Fig. 1, to provide many parameters for these variables in electronically accessible tables, and to check if they trace the Galactic Bar.

2 SELECTION OF VARIABLES

We used reddening maps published by Sumi (2003) for 48 OGLE-II Galactic Bulge fields. All variables of type A in a subset of these fields located at the Galactic latitude $b \approx -4^\circ$ are shown in Fig. 3. It is clear that they form three distinct groups: luminous red giants, less luminous red giants located near the Bulge red clump region, and relatively blue Galactic disc stars. These three groups are well separated. We selected stars located above and to the right of the line in Fig. 3 for our study, and we refer to them as OGLE Small Amplitude Red Giant variables (OSARGs).

Some type B variables are close to the saturation limit of OGLE-II, and therefore we restrict our study of the Galactic

structure to OSARG type A variables only. The OGLE saturation limit causes a problem for the study of the brightest OSARGs. This technical difficulty will be overturned when the ASAS I-band data (Pojmański 2002) become available, which have a limiting I-mag of about 14, and a considerable overlap with OGLE-II photometry. Three years of Galactic Bulge data have been acquired by ASAS already. For our analysis we omit fields located far from $b \approx -4^\circ$, and those fields for which a reliable extinction map is not available. This leaves us with a total of 33 OGLE-II fields.

3 DISTRIBUTION OF VARIABLES

The OSARG type A variables form a nearly horizontal sequence in the colour – magnitude diagram shown in Fig. 3. We fitted their distribution with a straight line using the least square method, and looking for the best global solution of the form:

$$I_{k,i,0} = I_{k,0} + a[(V - I)_{k,i,0} - 2.881], \quad (2)$$

where $I_{k,i,0}$ and $(V - I)_{k,i,0}$ are the reddening corrected average magnitude and colour for variable number i in the field k , $I_{k,0}$ is a constant, different for every field, representing the ‘average’ magnitude of OSARG type A variables in field k , a is the same constant for all fields, and 2.881 is the mean $(V - I)_0$ colour for all OSARG type A variables in all 33 fields represented in Fig. 3. We computed the value of the parameter a as 0.169. The values of the parameter $I_{k,0}$ and the standard deviations from the relation (2) are given in Table 1 for all 33 fields. This table also lists the total number of type A and type B variables in each field and the Galactic coordinates of the field centers.

Fig. 4 presents the variation of the average magnitude of OSARG type A variables with the Galactic longitude. A clear trend is present, practically identical to that shown by the red clump giants (Stanek et al. 1994, Stanek et al. 1997, Sumi 2003), demonstrating that OSARG variables are located in the Galactic Bar.

We repeated the analysis for OSARG type B variables and it was qualitatively similar to that shown in Fig. 4, but disturbed by the OGLE-II saturation limit.

4 MULTIPLE PERIODS

Multiple periods were detected for most OSARGs. The ratios of those periods to the dominant period (i.e., the one with the largest amplitude) are shown in Fig. 5 as a function of the dominant period. Several bands corresponding to the period ratios close to 2, 1.4, 0.9, 0.75, and 0.5 are clearly seen. The interpretation of this rich spectrum of oscillations is beyond the scope of our paper. Our intent is to present this richness with a hope that it may attract specialists to investigate the nature of the oscillations.

Virtually all OSARGs were identified with objects in the 2MASS catalogue, and the values of J, H, and K magnitude are included in the tables available on Internet/Simbad. A sample of these tables is shown in our Table 2. These magnitudes were corrected for interstellar extinction using maps developed by Sumi (2003) and using extinction ratios between the infrared bands and V-band provided by

Schlegel et al. (1998). Note that the extinction in K-band is small, and any errors in the estimate are of relatively little consequence. The average K-band magnitude, corrected for extinction, varies with Galactic longitude in a way similar to that seen in Fig. 4.

Next, extinction corrected K_0 magnitudes were also corrected for the Galactic Bar effect (as shown in Fig. 4 of this paper) to the distance corresponding to Galactic longitude $l = 0$; we label the corresponding magnitudes $K_{0,0}$. A relation between the dominant period of oscillations and $K_{0,0}$ is shown in Fig. 6. The two groups of OSARGs that are visible in Fig. 1 are also clearly visible in Fig. 6.

The two groups of OSARGs are also plotted in the infrared color – magnitude diagram in Fig. 7. Only 20% of all variables are plotted to avoid crowding. There is almost full overlap between the two groups, distinctly different from the clear separation in Fig. 1 and Fig. 6.

Fig. 8 shows the dependence of the dominant period on the reddening corrected $(V - I)_0$ color, and clear period – color relations are apparent. Note: K-band magnitude is close to the bolometric magnitude, and hence the period – luminosity relations are clearly visible in Fig. 6. However, the bright giants form a nearly horizontal line in the $I_0 - (V - I)_0$ diagram shown in Fig. 2. Hence, the $(V - I)_0$ color is for them a better absolute luminosity indicator than the I_0 magnitude, and this is clearly demonstrated in Fig. 8.

Finally, it is time for us to present a random sample of type A and type B OSARGs in Fig. 9. These are 12 variables of each type in the field BUL_SC3, sorted with increasing dominant period. These appear as semi-regular variables because of their rich period structure. A much longer time baseline of photometric measurements will become available soon when the current OGLE-III data are processed and published (cf. Udalski et al. 2002a). With a longer time baseline, it will be much easier to decide to what extent the multiple periods we found are stable, and to what extent OSARGs are multiply-periodic rather than semi-regular variables.

5 THE CATALOGUE

We provide a catalogue of 8970 OSARG type A variables and 6399 OSARG type B variables in electronic form at:

<http://www.astro.princeton.edu/~jwray/OSARG/>
in the files A.txt and B.txt, respectively. Separate files for each field are available at the same URL, and are called A1.txt, A2.txt, ..., A49.txt and B1.txt, B2.txt, ..., B49.txt. The catalogue is a subset of the general OGLE-II catalogue of variable stars in the Galactic Bulge (Woźniak et al. 2001). A sample of the tables, listing data for the first 25 type A stars from the field BUL_SC1, is shown in Table 2, which is split into two parts because of its considerable width. The consecutive columns are as follows: the variable star number according to Woźniak et al. (2001); the star number according to OGLE maps (Udalski et al. 2002b); 2000 RA and DEC; X and Y pixel coordinates; average V-band magnitude; V-band extinction; average $(V-I)$ color; $(V-I)$ reddening; average I-band magnitude; I-band extinction; J, H, K-band magnitudes; the dominant period and its amplitude; the next three significant periods and amplitudes. In cases where fewer than three significant periods were found, the

extra columns contain the value -99.99999. Similarly, for a few stars there was no match found in the 2MASS catalogue, so the J, H, K columns for those stars contain the value -9.999.

The coordinates and I and V-band magnitudes are given following OGLE maps (Udalski et al. 2002b), the reddening and extinction is given following Sumi (2003), and the J, H, K magnitudes are given following 2MASS (All-Sky Point Source Catalogue, Release 2003 March 25). We provide all these data in electronically accessible files to facilitate analysis of OSARG variables to all interested users.

6 DISCUSSION

There can be no doubt that OSARGs have been found in the MACHO database for the Galactic Bulge (Cook et al. 1997), and that they are related to red giant variables found in the LMC and SMC by Cook et al. (1997), by Kiss & Bedding (2003) and by Ita et al. (2003). However, there is also a striking difference between the Galactic Bulge and the LMC and SMC: the multiple narrow bands seen in the $\log P - K$ diagrams for the LMC and SMC are not present in the Galactic Bulge, where we see only two groups of stars. It appears that our type A and B variables correspond to type A⁻ and B⁻ variables, respectively, of Ita et al. (2003, fig. 6). Note: the distance modulus to the Galactic Bulge is 4 mag smaller than that to the LMC, so the red giant tip, which is at $K \approx 12$ in the LMC, is expected to be at $K \approx 8$ in the Galactic Bulge. Unfortunately, this is close to the I-band saturation limit of OGLE, and this complicates the comparison and biases our diagrams.

We have an impression that our two sequences of variables are broader in the apparent magnitude than the corresponding sequences seen in the LMC and SMC. This may be caused by at least two effects: the Galactic Bar has a relatively large radial depth, which remains an effect even after correction is made for the inclination (cf. Fig. 4), and there is likely also a broad range of metallicities in our Galaxy as compared to LMC and SMC.

Another striking difference between OSARGs and similar variables in the LMC is the presence of a large number of LMC stars with color $(J - K) > 1.4$, as shown in fig. 3 of Kiss & Bedding (2003); these are carbon stars. We found very few such variables, as is apparent in our Fig. 7, where there are less than a handful of stars off the right hand limit of the figure. This difference may be due to the higher metallicity of the Galactic Bulge as compared with the LMC.

The period – amplitude relations as presented in our Fig. 1 have not been reported in print to the best of our knowledge. However, similar relations were found for the LMC and SMC variables by Soszyński (2003).

We restrict this paper to the announcement of the OSARG variables in the Galactic Bulge/Bar, to the catalogue of 15,369 objects, and to the demonstration that they are located in a bar inclined to the line of sight. We make no attempt at modelling the Bar, as considerably more complete data should be available as soon as ASAS photometry (cf. Pojmański 2002) becomes available, and the problems with the OGLE saturation limit are alleviated.

ACKNOWLEDGMENTS

This work was supported with the NSF grant AST-0204908, and NASA grant NAG5-12212. This publication makes use of data products from the Two Micron All Sky Survey, which is a joint project of the University of Massachusetts and the Infrared Processing and Analysis Center/California Institute of Technology, funded by the National Aeronautics and Space Administration and the National Science Foundation

REFERENCES

- Blitz L., Spergel D. N., 1991, *ApJ*, 379, 631
 Christensen-Dalsgaard J., Kjeldsen H., Mattei J. A., 2001, *ApJ*, 562, L141
 Cook K. H. et al. (MACHO), 1997, in Ferlet R., Maillard J.-P., Raban B., eds, 12th IAP Astrophysics Meeting, Variable stars and the astrophysical returns of microlensing surveys. Editions Frontières, Gif-sur-Yvette p. 17
 Dehnen W., 2002, in Athanassoula E., Bosma A., Mujica R., eds, ASP Conf. Ser. 275, Disks of Galaxies: Kinematics, Dynamics and Perturbations. Astron. Soc. Pac., San Francisco, p. 105
 de Vaucouleurs G., 1964, in Kerr F. J., Rodgers A. W., eds, Proc. IAU Symp. 20, The Galaxy and the Magellanic Clouds. (Canberra: Australian Acad. Sci.), p. 195
 Dziembowski W. A. et al., 2001, *MNRAS*, 328, 601
 Eyer L., Grenon M., 1997, *ESA SP-402*, 467
 Eyer L., Blake C., 2002, in Aerts C., Bedding T. R., Christensen-Dalsgaard J., eds, ASP Conf. Ser. 259, Radial and Nonradial Pulsations as Probes of Stellar Physics. Astron. Soc. Pac., San Francisco, p. 160
 Garzón F., 1999, in Beckman J. E., Mahoney T. J., eds, ASP Conf. Ser. 187, The Evolution of Galaxies on Cosmological Timescales. Sheridan Books, San Francisco, p. 31
 Gerhard O., 2002, in Da Costa G. S., Jerjen H., eds, ASP Conf. Ser. Vol. 273, The Dynamics, Structure and History of Galaxies: A Workshop in Honour of Prof. K. Freeman. Astron. Soc. Pac., San Francisco, p. 73
 Glass I. S., Schultheis M., 2003, preprint (astro-ph/0307366)
 Ita Y. et al., 2003, preprint (astro-ph/0310083)
 Jorissen A. et al., 1997, *A&A*, 324, 578
 Kiss L. L., Bedding T., 2003, *MNRAS*, 343, L79
 Lomb N. R., 1976, *Ap&SS*, 39, 447
 Matsumoto T. et al., 1982, in Riegler G., Blandford R., eds, The Galactic Center. American Institute of Physics, New York, p. 48
 Merrifield M. R., 2003, preprint (astro-ph/0308302)
 Nakada Y. et al., 1991, *Nature*, 353, 140
 Pojmański G., 2002, *AcA*, 52, 397
 Press W. H. et al., 1992, Numerical recipes in Fortran. Cambridge University Press
 Schlegel D., Finkbeiner D. P., Davis M., 1998, *ApJ*, 500, 525
 Soszyński I. (OGLE), 2003, PhD Thesis, Warsaw University
 Stanek K. Z. et al. (OGLE), 1994, *ApJ*, 429, L73
 Stanek K. Z. et al. (OGLE), 1997, *ApJ*, 477, 163
 Sumi T., 2003, preprint (astro-ph/0309206)
 Udalski A. et al. (OGLE), 1992, *AcA*, 42, 253
 Udalski A., Kubiak M., Szymański M. (OGLE), 1997, *AcA*, 47, 319
 Udalski A. et al. (OGLE), 2002a, *AcA*, 52, 1
 Udalski A. et al. (OGLE), 2002b, *AcA*, 52, 217
 Wood P. R. et al. (MACHO), 1999, in Le Bertre T., Lebre A., Waelkens C., eds, Proc. IAU Symp. 191, Asymptotic giant branch stars. Astron. Soc. Pac., San Francisco, p. 151
 Wood P. R., 2000, *Publ. Astr. Soc. Australia*, 18, 18
 Woźniak P. R. et al. (OGLE), 2001, *AcA*, 51, 175

Table 1. Values for 33 fields of the reddening corrected average magnitude $I_{k,0}$ and its rms, as well as the Galactic longitude l and latitude b of the field centers, and the number of A and B stars, N_A , N_B .

Field k	l	b	N_A	N_B	$I_{k,0}$	rms
1	1.08	-3.62	225	136	11.91	0.36
2	2.23	-3.46	204	133	11.92	0.41
8	10.48	-3.78	39	32	11.84	0.52
9	10.59	-3.98	34	27	11.59	0.66
10	9.64	-3.44	16	17	12.00	0.62
11	9.74	-3.64	15	20	11.57	0.45
12	7.80	-3.37	84	55	11.84	0.55
13	7.91	-3.58	21	22	11.75	0.47
16	5.10	-3.29	92	92	11.79	0.47
17	5.28	-3.45	93	91	11.91	0.48
18	3.97	-3.14	197	108	11.89	0.46
19	4.08	-3.35	181	121	11.79	0.45
20	1.68	-2.47	422	257	11.96	0.43
21	1.80	-2.66	337	179	11.97	0.42
22	-0.26	-2.95	294	197	12.01	0.41
23	-0.50	-3.36	224	175	11.94	0.42
24	-2.44	-3.36	120	150	12.14	0.43
25	-2.32	-3.56	154	109	12.05	0.40
26	-4.90	-3.37	174	113	12.07	0.35
27	-4.92	-3.65	164	102	12.05	0.43
28	-6.76	-4.42	57	40	12.10	0.40
29	-6.64	-4.62	68	46	12.04	0.41
30	1.94	-2.84	321	196	11.96	0.40
31	2.23	-2.94	313	157	11.93	0.43
32	2.34	-3.14	261	137	11.94	0.40
33	2.35	-3.66	174	116	11.95	0.40
34	1.35	-2.40	387	275	11.95	0.43
35	3.05	-3.00	216	146	11.87	0.41
36	3.16	-3.20	214	138	11.95	0.42
38	0.97	-3.42	195	160	11.94	0.41
40	-2.99	-3.14	214	154	12.03	0.43
41	-2.78	-3.27	196	174	12.09	0.35
42	4.48	-3.38	158	130	11.82	0.47

Table 2. Table of all relevant parameters for a sample of type A stars in field 1.

NoV	NoS	RA	DEC	X-p	Y-p	V	A(V)	(V-I)	E(V-I)	I	A(I)
7	43	18:02:09.55	-30:25:14.8	311.41	97.78	17.640	1.558	4.436	0.793	13.195	0.765
17	189902	18:02:20.02	-30:25:44.1	638.85	27.45	15.906	1.612	3.973	0.820	11.926	0.791
67	47	18:02:04.36	-30:24:37.1	148.87	188.64	16.774	1.720	3.570	0.876	13.199	0.844
91	189911	18:02:23.19	-30:24:45.9	737.63	168.23	17.812	1.746	4.944	0.889	12.859	0.857
136	554673	18:02:52.20	-30:24:36.9	1644.51	191.09	16.042	1.595	2.906	0.812	13.130	0.783
149	19	18:02:03.70	-30:23:44.5	127.99	315.63	14.878	1.700	2.571	0.865	12.304	0.834
154	15	18:02:08.06	-30:24:08.8	264.47	257.18	15.898	1.731	2.873	0.881	13.020	0.850
176	189919	18:02:29.47	-30:23:59.4	933.64	280.90	16.641	1.569	3.710	0.799	12.924	0.770
206	554654	18:02:50.62	-30:23:48.5	1594.97	307.91	17.204	1.552	4.524	0.790	12.672	0.762
212	554680	18:03:00.55	-30:24:05.9	1905.53	266.15	17.325	1.708	4.225	0.870	13.091	0.839
226	66	18:02:04.59	-30:22:54.4	155.33	436.61	16.938	1.637	3.511	0.833	13.421	0.804
230	29	18:02:07.99	-30:22:39.8	261.73	472.18	16.046	1.628	3.630	0.829	12.410	0.799
251	189976	18:02:31.04	-30:22:45.9	982.43	458.63	15.787	1.521	2.614	0.775	13.169	0.747
261	376353	18:02:35.57	-30:22:33.2	1123.94	489.42	16.818	1.489	4.165	0.758	12.645	0.731
312	201645	18:02:19.74	-30:22:06.3	628.98	553.78	15.425	1.547	2.822	0.787	12.598	0.759
313	201647	18:02:20.07	-30:21:38.4	639.17	621.36	16.116	1.718	3.210	0.875	12.901	0.844
328	387446	18:02:41.92	-30:21:38.7	1322.35	621.36	17.307	1.556	4.577	0.792	12.722	0.764
343	565509	18:02:52.41	-30:21:54.6	1650.68	583.25	15.576	1.728	3.126	0.879	12.443	0.848
344	565507	18:02:52.69	-30:21:57.7	1659.37	575.75	15.713	1.728	2.848	0.879	12.860	0.848
368	11929	18:02:06.27	-30:20:46.1	207.04	746.77	16.164	1.779	3.430	0.906	12.728	0.874
395	201653	18:02:18.83	-30:20:59.4	600.22	715.45	14.756	1.681	2.491	0.856	12.260	0.825
403	201655	18:02:31.71	-30:20:53.9	1002.91	729.26	16.301	1.517	3.735	0.772	12.560	0.745
438	565514	18:03:00.60	-30:20:59.3	1906.77	717.13	15.725	1.595	3.669	0.812	12.048	0.783
454	201665	18:02:16.25	-30:19:51.0	518.93	880.53	15.038	1.706	2.543	0.868	12.490	0.837
463	201663	18:02:20.67	-30:20:00.5	657.37	857.82	15.540	1.711	2.870	0.871	12.664	0.840

NoV	J	H	K	Pd.1	Amp.1	Pd.2	Amp.2	Pd.3	Amp.3	Pd.4	Amp.4
7	10.629	9.613	9.216	19.9844	0.01798	-99.9999	-99.9999	-99.9999	-99.9999	-99.9999	-99.9999
17	9.711	8.686	8.296	32.5068	0.03572	-99.9999	-99.9999	-99.9999	-99.9999	-99.9999	-99.9999
67	11.097	10.041	9.649	20.6378	0.00881	-99.9999	-99.9999	-99.9999	-99.9999	-99.9999	-99.9999
91	9.730	8.688	8.196	36.7674	0.04686	504.9388	0.03138	50.4939	0.02320	291.3108	0.02110
136	11.247	10.222	9.937	20.8652	0.00998	27.1472	0.00978	20.1976	0.00635	59.6384	0.00597
149	10.523	9.561	9.261	17.2138	0.00727	236.6901	0.00572	-99.9999	-99.9999	-99.9999	-99.9999
154	11.165	10.141	9.776	13.3582	0.00566	1262.3469	0.00537	-99.9999	-99.9999	-99.9999	-99.9999
176	10.737	9.760	9.350	18.9827	0.01322	-99.9999	-99.9999	-99.9999	-99.9999	-99.9999	-99.9999
206	10.001	8.953	8.538	29.8192	0.04676	51.5244	0.02070	504.9388	0.01790	75.7408	0.01323
212	10.587	9.544	9.129	20.4153	0.01291	-99.9999	-99.9999	-99.9999	-99.9999	-99.9999	-99.9999
226	11.308	10.305	9.906	18.5185	0.01553	315.5867	0.00866	-99.9999	-99.9999	-99.9999	-99.9999
230	10.294	9.291	8.924	22.8135	0.01736	33.0746	0.01281	46.7536	0.01207	541.0058	0.01264
251	11.433	10.475	10.160	14.2907	0.00574	27.2449	0.00533	-99.9999	-99.9999	-99.9999	-99.9999
261	10.095	9.103	8.696	23.2259	0.02700	22.7332	0.01737	-99.9999	-99.9999	-99.9999	-99.9999
312	10.768	9.750	9.426	20.3604	0.01763	29.1311	0.00832	18.5639	0.00644	-99.9999	-99.9999
313	10.920	9.894	9.532	20.5260	0.00979	28.6897	0.00775	-99.9999	-99.9999	-99.9999	-99.9999
328	9.947	8.956	8.453	28.7988	0.02869	541.0058	0.01892	-99.9999	-99.9999	-99.9999	-99.9999
343	10.529	9.556	9.160	15.8454	0.00857	12.2558	0.00615	-99.9999	-99.9999	-99.9999	-99.9999
344	11.004	10.048	9.727	14.9982	0.00580	-99.9999	-99.9999	-99.9999	-99.9999	-99.9999	-99.9999
368	10.675	9.631	9.260	23.8179	0.01882	473.3801	0.01516	176.1414	0.01160	34.7435	0.01090
395	10.585	9.598	9.250	16.5373	0.00668	118.3450	0.00578	-99.9999	-99.9999	-99.9999	-99.9999
403	10.374	9.295	8.879	28.5814	0.01643	40.2877	0.01585	541.0059	0.01578	-99.9999	-99.9999
438	9.933	8.933	8.575	26.4828	0.01878	445.5342	0.01378	38.8414	0.01258	27.7439	0.01009
454	10.750	9.733	9.440	17.8634	0.00683	34.5848	0.00617	-99.9999	-99.9999	-99.9999	-99.9999
463	10.782	9.756	9.314	18.5185	0.00890	582.6217	0.00719	24.0447	0.00534	-99.9999	-99.9999

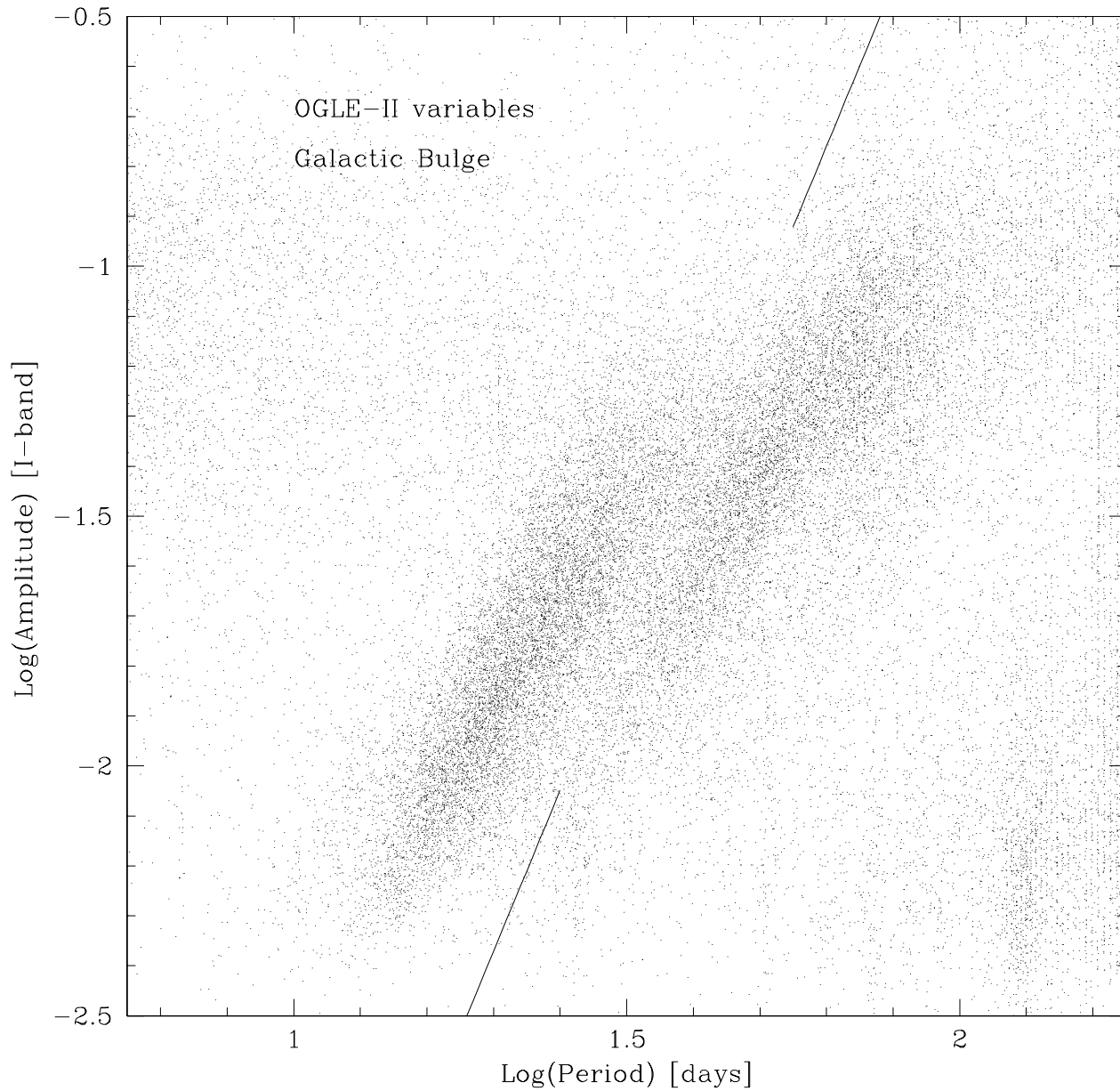


Figure 1. The period – amplitude diagram is shown for $\sim 200,000$ OGLE-II variables in the Galactic Bulge. Two sequences, separated by two segments of diagonal solid line, are clearly visible. We call the sequence above and to the left of the line type A, and the sequence below and to the right of the line we call type B. A cluster of points at $\log P \approx 2.1$ and $\log A \approx -2.3$ is an artefact to be ignored. Amplitudes are defined as half of the peak-to-peak amplitude for a given mode.

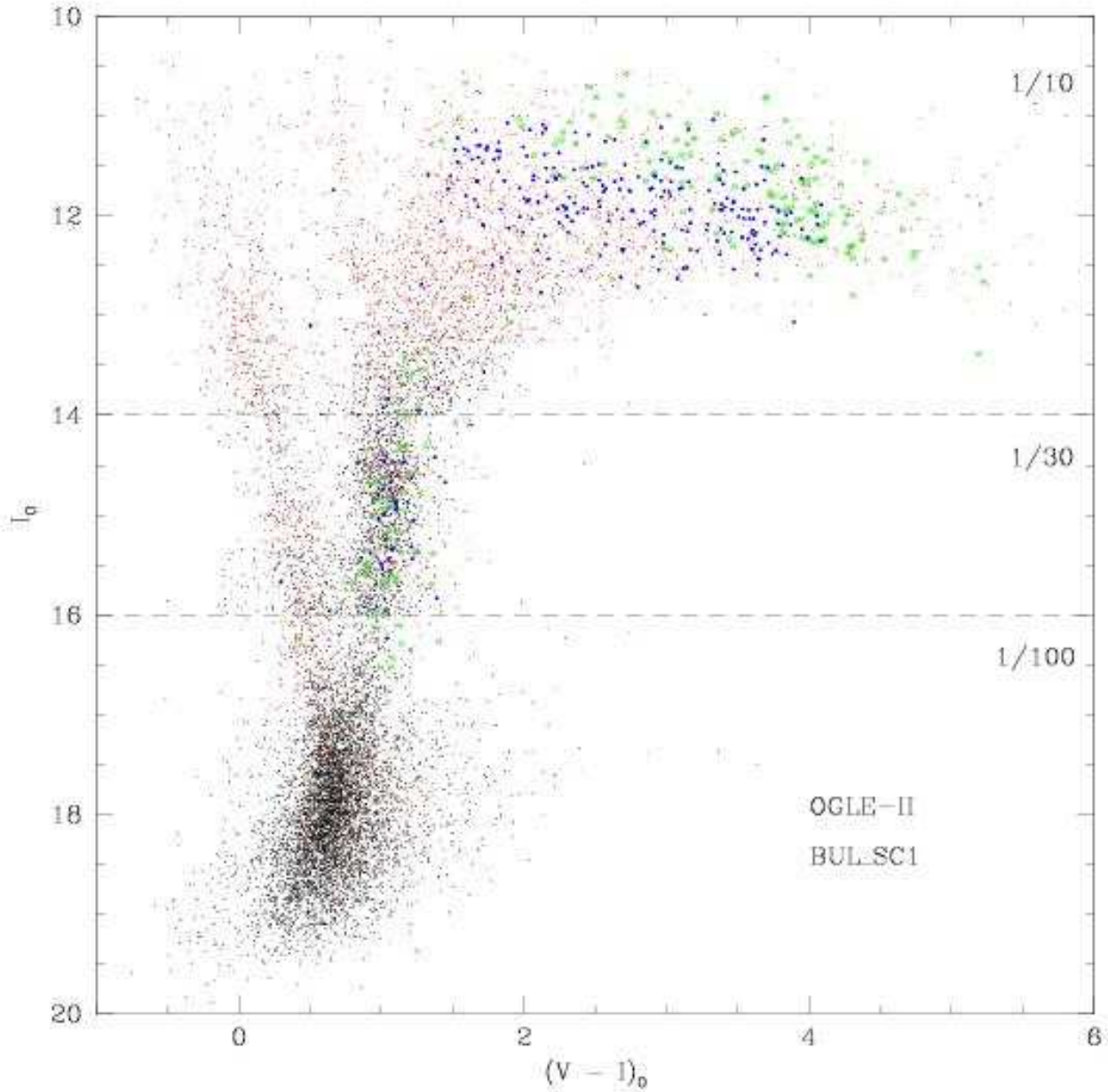


Figure 2. The extinction and reddening corrected colour – magnitude diagram $I_0 - (V - I)_0$ is shown for type A (large blue dots) and type B (green open circles) variables in the OGLE-II field BUL_SC1. Small red points represent other variables. Small black points represent non-variable stars. In the three sections of the diagram, separated by horizontal dashed lines, the fraction of non-variable stars plotted is as indicated: 1/10, 1/30, and 1/100, from top to bottom.

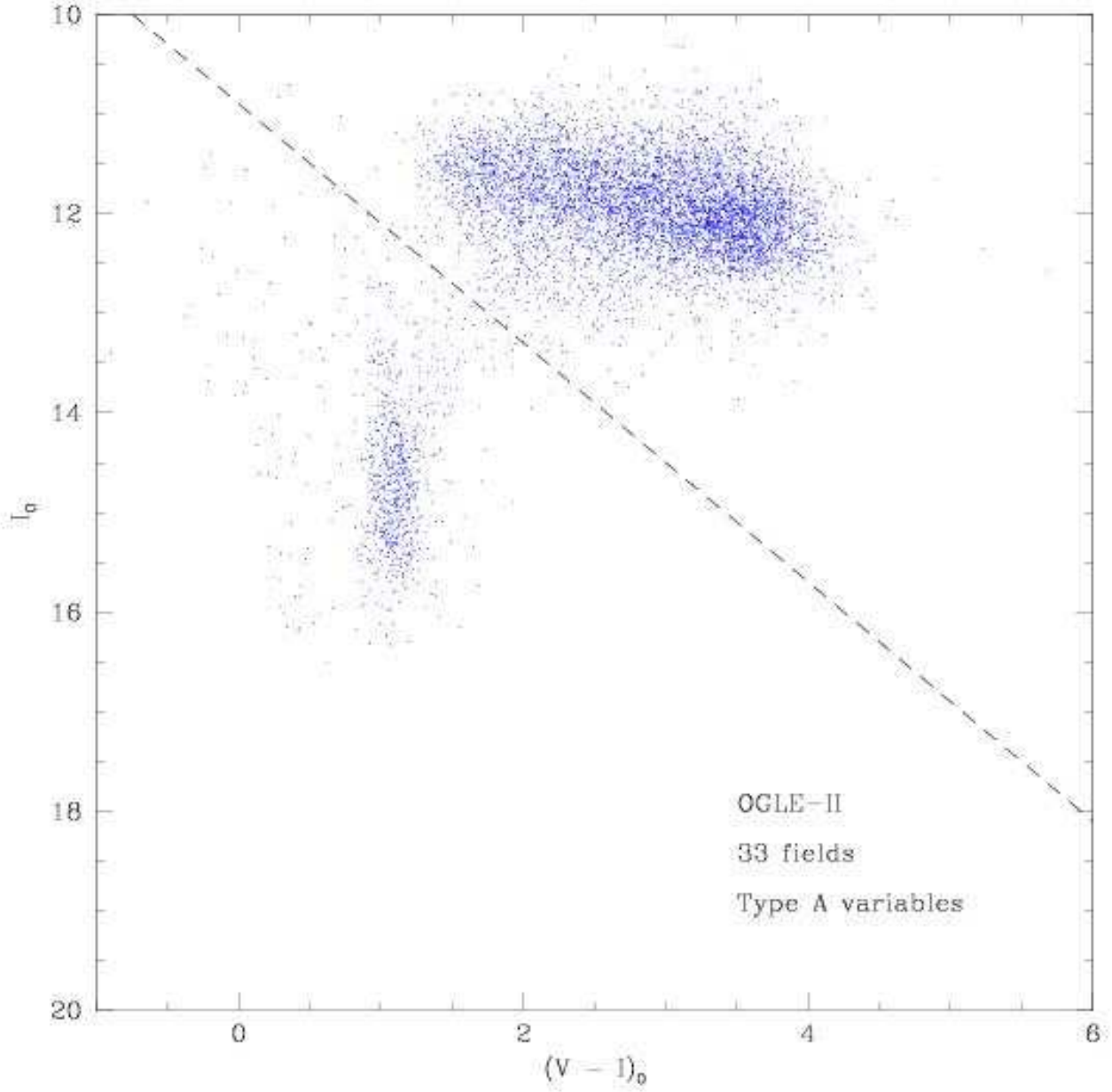


Figure 3. The extinction and reddening corrected colour – magnitude diagram $I_0 - (V - I)_0$ is shown for type A variables in 33 OGLE-II fields. The variables to be discussed in this paper are located above and to the right of the diagonal dashed line.

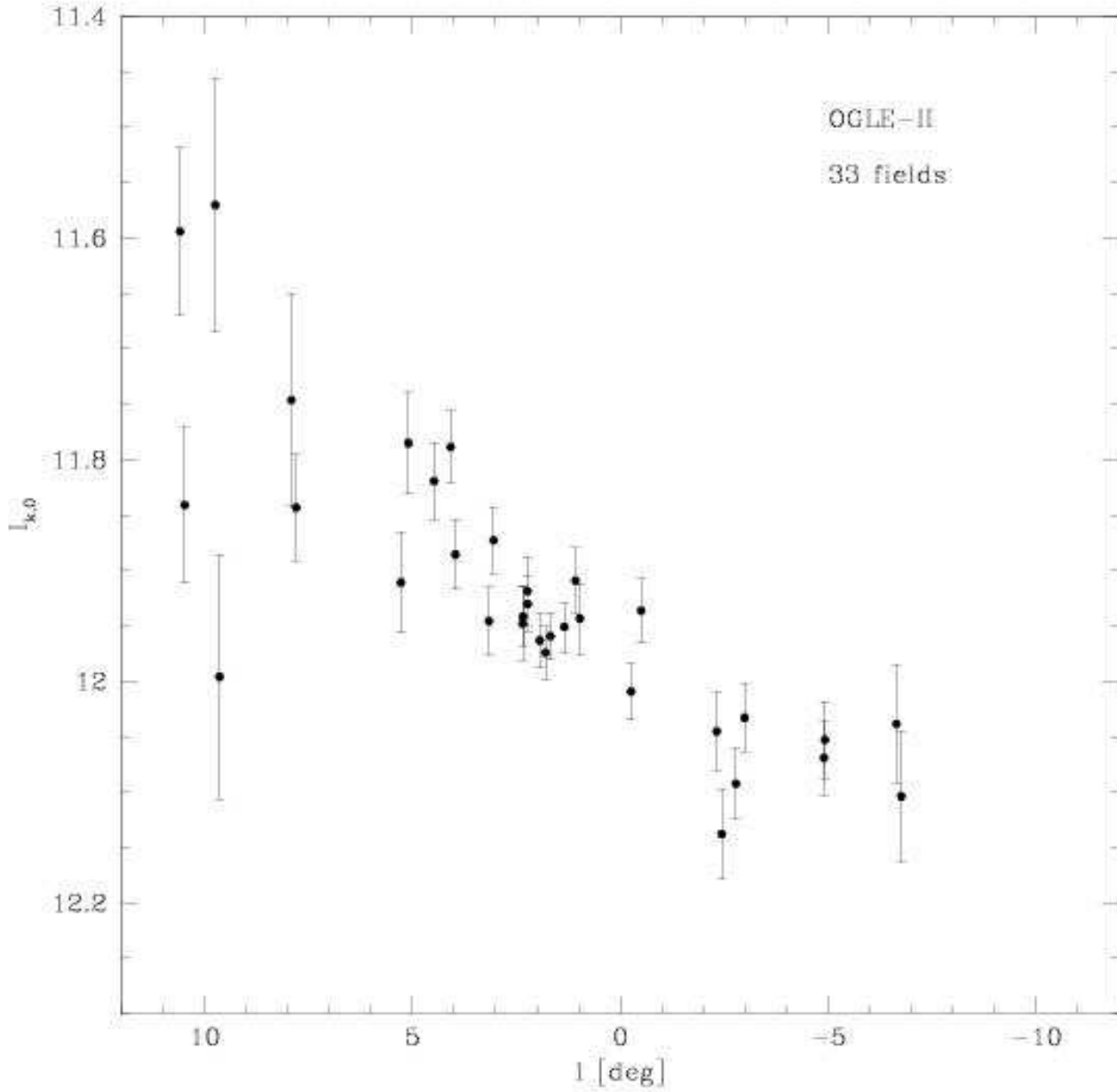


Figure 4. The reddening corrected average I-band magnitude for OSARG type A variables in 33 OGLE-II fields is shown as a function of Galactic longitude l .

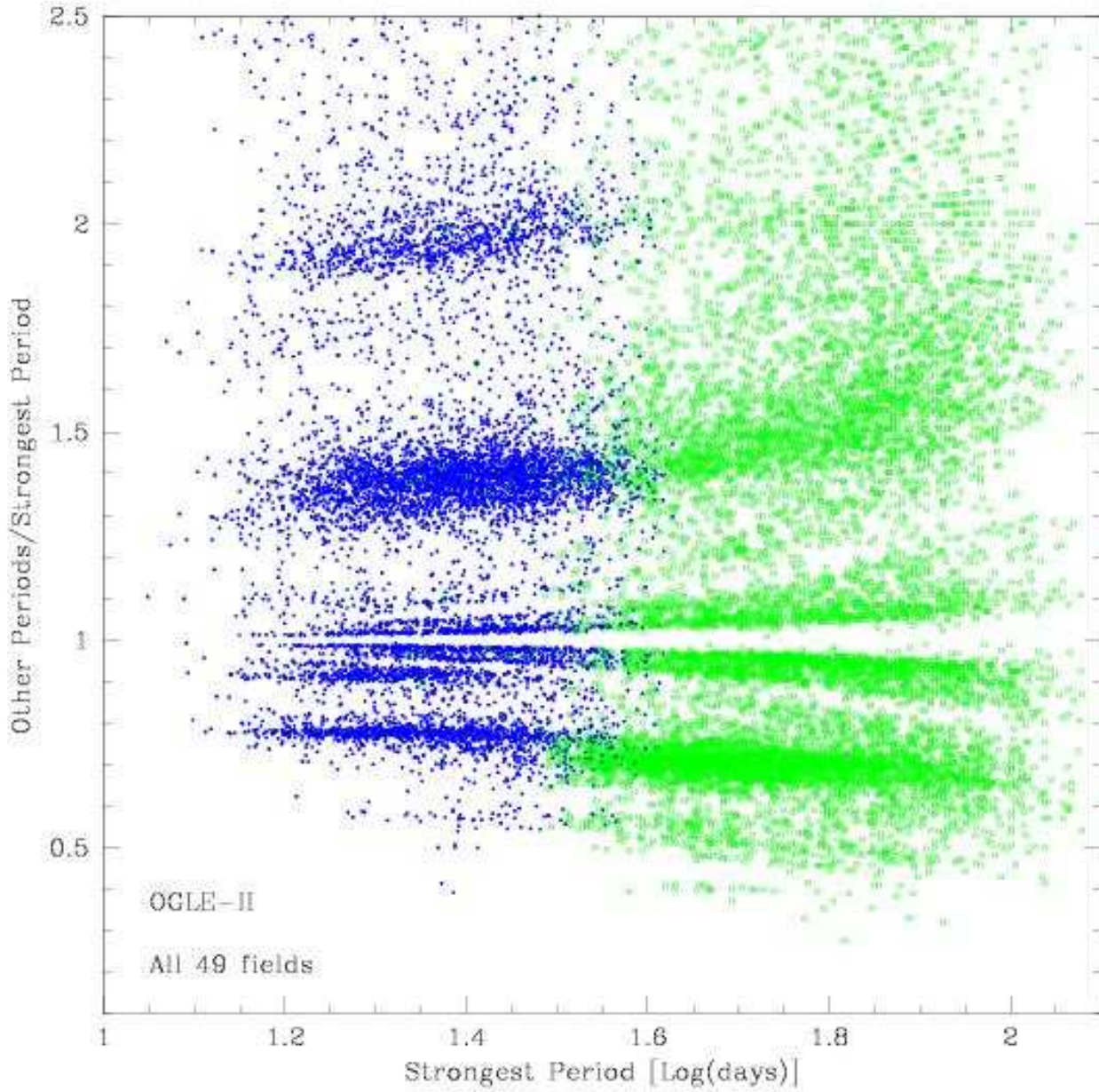


Figure 5. The ratios of all significant periods to the dominant period are shown as a function of the dominant period for all OSARG variables, type A (blue points) and type B (green open circles).

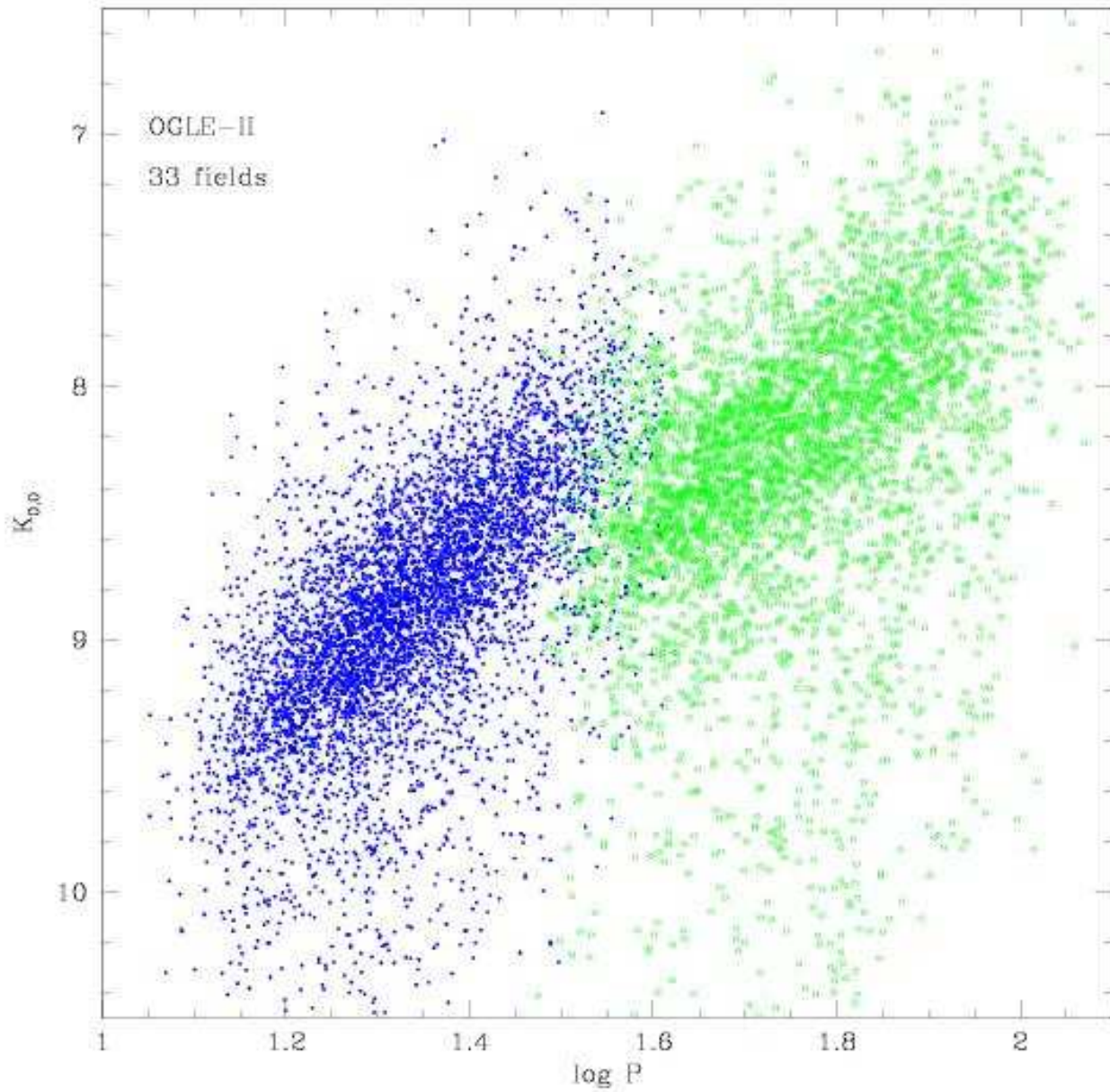


Figure 6. The period – luminosity diagram for OSARGs in K-band. The K-band magnitude of all OSARG variables was obtained from 2MASS and corrected for the interstellar extinction and the difference in distance induced by the Galactic Bar (cf. Fig. 4 of this paper), yielding $K_{0,0}$, which is shown as a function of the dominant period. Note the clear separation of the two types of OSARG variables, type A (blue points) and type B (green open circles).

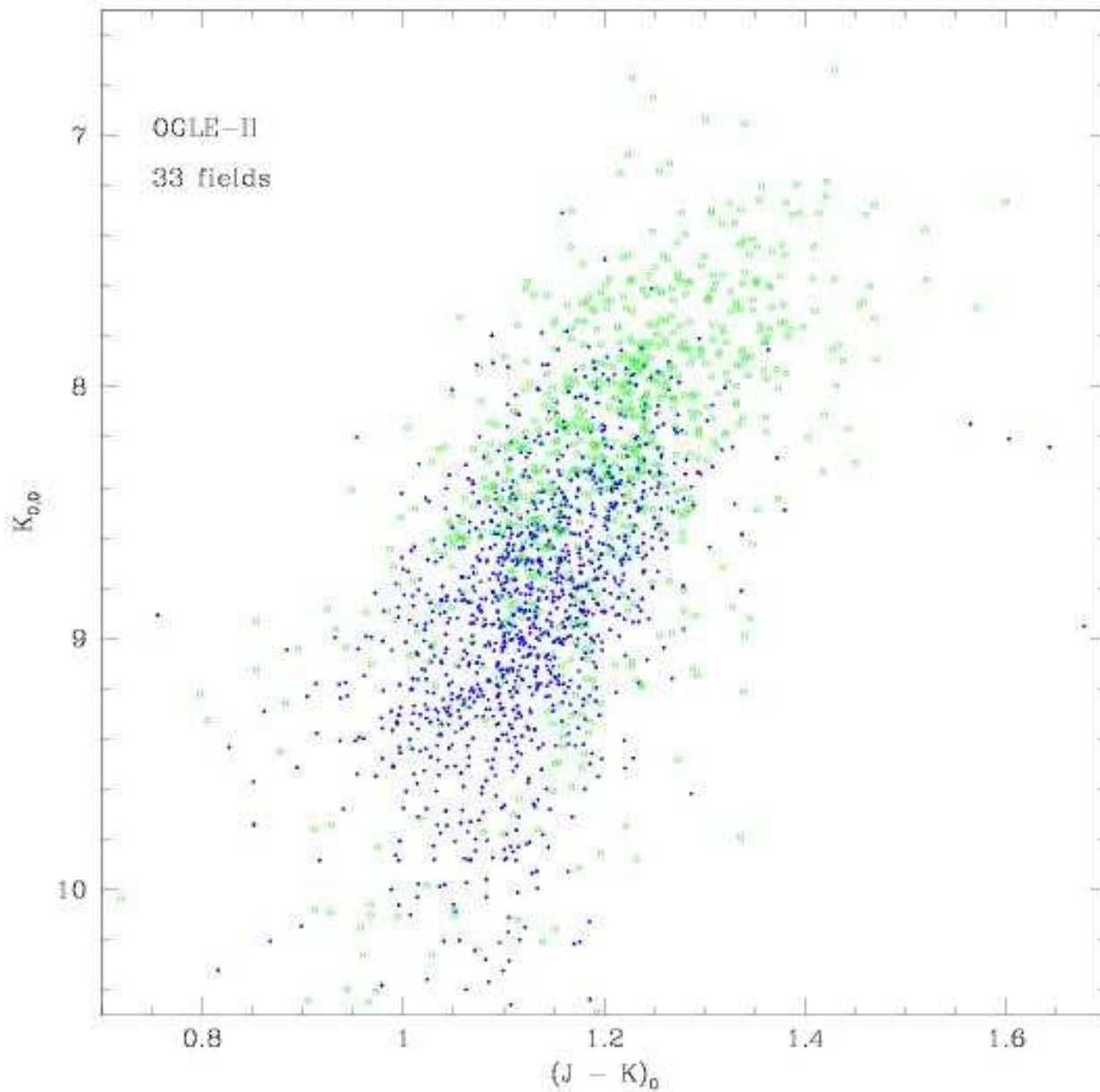


Figure 7. The infrared colour – magnitude diagram for OSARGs based on 2MASS J and K magnitudes corrected for the interstellar extinction and, in the case of $K_{0,0}$, also for the Galactic Bar-induced difference in distance, as determined from Fig. 4 of this paper. Only 20% of all variables are plotted to avoid crowding. Notice that type A OSARGs (blue points) and type B OSARGs (green open circles) overlap in some area of the CMD.

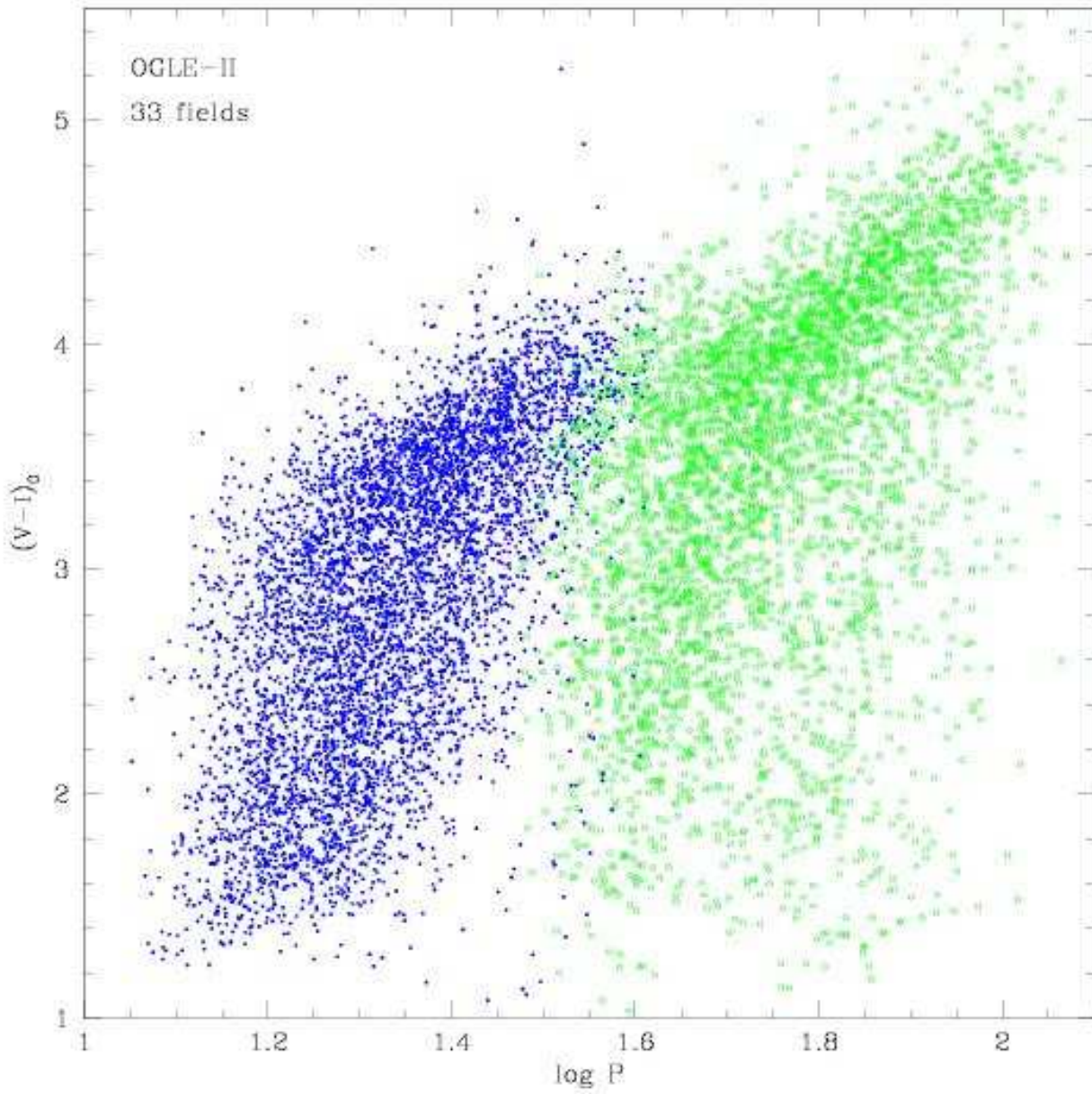


Figure 8. The reddening corrected $(V-I)_0$ colour as a function of the dominant period. Two distinct period – colour relations, for type A (blue points) and for type B (green open circles), are clearly apparent.

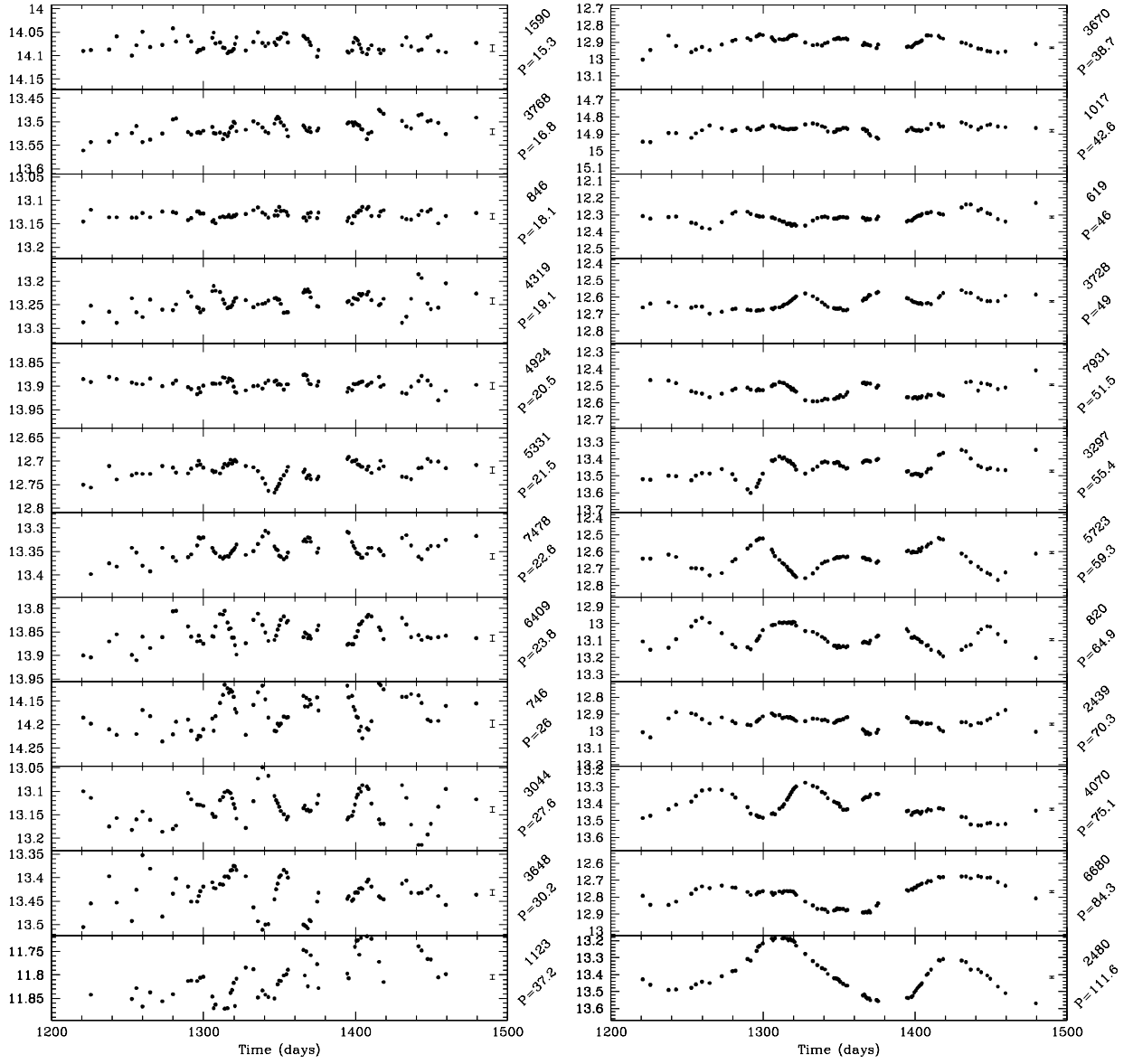


Figure 9. A sample of light curves with periods (in days) increasing from top to bottom, for type A (left) and type B (right) variables.